Stochasticity directs adaptive evolution toward transient evolutionary attractors

Type of article: Letter

Short title: Transient evolutionary attractors

John P. DeLong*[1] and Clayton E. Cressler*[1]

[1]School of Biological Sciences, University of Nebraska – Lincoln, Lincoln, NE, 68588, USA

*Co-corresponding authors

ORCID for JPD: 0000-0003-0558-8213

ORCID for CEC: 0000-0002-6281-2798

Statement of authorship: Both authors conceived of the idea and performed modeling analyses. JPD wrote the first draft of the manuscript, and both authors contributed substantially to revisions.

Data accessibility statement: We confirm that, should the manuscript be accepted, the code supporting the results will be archived in an appropriate public repository. No new data were used in the manuscript.

Number of words in the abstract: 149

Number of words in the main text: 4950

Number of references: 78

Number of figures: 4

Number of tables: 0

Number of text boxes: 0

Keywords: stochastic dynamics, eco-evolutionary dynamics, GEM, Gillespie algorithm, maladaptation, harvest induced evolution

Abstract

Stochastic processes such as genetic drift may hinder adaptation, but the effect of such stochasticity on evolution via its effect on ecological dynamics is poorly understood. Here we evaluate patterns of adaptation in a population subject to variation in demographic stochasticity. We show that stochasticity can alter population dynamics and lead to evolutionary outcomes that are not predicted by classic eco-evolutionary modeling approaches. We also show, however, that these outcomes are governed by transient evolutionary attractors (TEAs) – these are maxima in lifetime reproductive success when the ecological system is not at equilibrium. These TEAs alter the path of evolution but are not visible through the equilibrium lens that underlies much evolutionary theory. We further show that trait-independent culling can redirect evolution away from expected evolutionary equilibria and toward these TEAs. Our results reveal that considering population processes during transient periods can greatly improve our understanding of the path and pace of evolution.

Introduction

Debates over the effects of stochasticity on ecological and evolutionary dynamics go back to foundational work in ecology and evolutionary biology, from Fisher's and Wright's contrasting views of the role of mutation and drift (Fisher 1930; Wright 1931) to Nicholson's and Andrewartha and Birch's differing opinions about whether populations were primarily regulated by density-dependent or density-independent (e.g., stochastic) processes (Andrewartha & Birch 1954; Nicholson 1957). Mathematical models have proven to be a valuable tool for studying the various ways that stochasticity can impact ecological (reviewed in Coulson *et al.* 2004; Black & McKane 2012) and evolutionary (reviewed in Lenormand *et al.* 2009) dynamics. For example, evolutionary theory has revealed the potential for genetic drift to facilitate adaptation (Wright's "shifting balance" theory; Wright 1931, Coyne et al. 1997) and how stochasticity can shape life history evolution (e.g., "bet hedging" strategies; Cohen 1966; Childs *et al.* 2010; Rees & Ellner 2019). Ecological theory has shown how stochasticity can excite an underlying deterministic tendency for a system to oscillate, leading to sustained oscillations (Greenman & Benton 2003; McKane & Newman 2005), and how it can cause systems to shift between different deterministic attractors (Henson *et al.* 1998; Ives *et al.* 2008; Ashwin *et al.* 2012; Abbott & Nolting 2017). However, despite this long-standing interest, there is a need for additional work studying how stochasticity affects evolutionary dynamics *through* its effects on ecological dynamics.

A number of theoretical approaches for studying the interplay between ecological and evolutionary dynamics have been proposed (reviewed in Abrams 2001), including quantitative genetics (QG) and adaptive dynamics (AD) approaches (Abrams *et al.* 1993b; Dieckmann & Law 1996; Geritz *et al.* 1998; Abrams 2001). While there are important differences between the two methods, for example in their assumptions about reproduction and the relative timescales of ecological and evolutionary processes, their predictions for eco-evolutionary dynamics are often identical. This is because, in both approaches, the direction of selection is determined by the fitness gradient: the derivative of individual

fitness (W) with respect to the evolving trait (x) (Abrams *et al.* 1993b; Abrams 2001; Doebeli *et al.* 2017). The dynamics of the mean trait ($\bar{x}$) are given by:

$$\frac{d\bar{x}}{dt} \propto \left(\frac{\partial W}{\partial x}\right)_{x=\bar{x}}.$$

An equation of this form can be arrived at either through the equations for trait change in quantitative genetics (Lande 1976; Abrams *et al.* 1993b) or through a simplification of the master equation of a stochastic birth-death process (Dieckmann & Law 1996). Given that individual fitness will be affected by ecological interactions, there is broad scope for eco-evolutionary feedbacks to affect the dynamics of both the ecological and evolutionary system (Fussmann *et al.* 2003; Cortez & Ellner 2010; Vasseur *et al.* 2011; Cortez 2016; Lowe *et al.* 2017).

Given the key role of ecological dynamics in shaping the fitness gradient, stochasticity that alters ecological dynamics also may influence adaptation (Lowe *et al.* 2017; Start *et al.* 2020). However, both the QG and AD approaches typically assume that populations are large so that demographic stochasticity (random variation in the sequence and number of demographic events) can safely be ignored. Studies that have included demographic stochasticity have shown that it can alter the eco-evolutionary dynamics predicted by QG and AD approaches (Proulx & Day 2001). For example, demographic stochasticity can affect the dynamics of adaptation through genetic drift (Lenormand *et al.* 2009), the loss of high-fitness genotypes (Crespi 2000), delaying or preventing evolutionary branching due to disruptive selection (Claessen *et al.* 2007; Wakano & Iwasa 2013), or leading to the evolution of pathogens with lower transmission rates and virulence (Humplik *et al.* 2014; Parsons *et al.* 2018).

In addition, demographic heterogeneity (differences in expected demographic rates among individuals) may influence evolutionary outcomes through two mechanisms. First, variation in traits among individuals can affect ecological and evolutionary dynamics, even if those differences are not heritable (Bolnick *et al.* 2011; Kendall *et al.* 2011; Stover *et al.* 2012a; Cressler *et al.* 2017). Second, when trait differences do lead to differences in the expected fitness of those individuals (Figure 1A),

demographic stochasticity causes individuals to randomly deviate from their expected fitness, which is known as individual demographic stochasticity (van Daalen & Caswell 2017). For example, Banks & Thompson (1987) assessed lifetime reproductive success of the damselfly *Coenagrion puella* with respect to individual head width (Figure 1B). Although there was a range of fitness-maximizing values of head width in the damselfly population, the realized lifetime reproductive success of individuals was quite variable, and many individuals with an optimal head width realized relatively low fitness (Figure 1B).

An outstanding question is whether approaches to studying trait dynamics, such as QG and AD, that do not consider the effects of demographic stochasticity can still provide insight into trait evolution when it is present and alters ecological dynamics. To answer this question, here we use Gillespie eco-evolutionary models [GEMs] (DeLong & Gibert 2016; DeLong & Luhring 2018; DeLong & Belmaker 2019) to generate ecological and evolutionary dynamics through the simulation of stochastic birth-death processes (Dieckmann & Law 1996; Champagnat *et al.* 2006; Doebeli *et al.* 2017). Specifically, we compare the ecological and evolutionary dynamics produced by GEMs to deterministic expectations based on the quantitative genetics (QG) approach (Lande 1976; Abrams *et al.* 1993b). We study the eco-evolutionary dynamics of a simple ecological model of logistic growth in two scenarios: 1) varying the location of the ecological equilibrium (i.e., carrying capacity) and 2) introducing additional mortality (e.g., culling) that is unrelated to an individual's traits. Importantly, we find that the realized evolutionary outcome can still be understood using the deterministic equations underlying population growth and the expected values of fitness, even when demographic stochasticity prevents populations from reaching the expected eco-evolutionary equilibrium. In particular, we show that demographic stochasticity often causes the population size to be smaller than the deterministic expectation, which can trap populations at "transient evolutionary attractors" (TEAs). TEAs are trait values that maximize lifetime reproductive success, given the non-equilibrium population size induced by stochasticity or

other trait-independent forces acting on abundance, and can be calculated from the deterministic equations governing births and deaths. We suggest that these TEAs may play an important role driving evolutionary dynamics in many natural systems, and more generally, that understanding transient evolutionary phenomenon may provide new insights into how populations evolve.

Material and methods

Deterministic eco-evolutionary dynamics: The quantitative genetics approach to modeling eco-evolutionary dynamics allows for ecological and evolutionary dynamics to occur on similar timescales (Abrams 2001). The QG approach derives the fitness gradient equation as an approximation of the quantitative genetics equations of Lande (1976) that assume that the trait distribution is unimodal and that the variance in fitness is greater than the variance in the trait (Iwasa *et al.* 1991; Taper & Case 1992; Abrams *et al.* 1993a, b; Abrams 2001). An identical expression also can be derived from the dynamics of genotypes via the Price equation (Taylor & Day 1997; Day & Gandon 2006; Queller 2017). The rate of evolutionary change is also affected by the additive genetic variance; this value is often held constant but can be allowed to change dynamically (Abrams et al. 1993b, Taylor & Day 1997, Tirok *et al.* 2011).

To investigate how stochasticity influences evolutionary dynamics, we consider a simple model for density-dependent population growth that can provide deterministic baseline expectations:

$$\frac{dR}{dt} = (b_{max} - b_s R)R - (d_{min} + d_s R)R, \qquad \text{(Equation 1)}$$

where R is population abundance, b_{max} is the maximum birth rate, d_{min} is the minimum death rate, and b_s and d_s characterize the effects of population abundance on the realized birth and death rates, respectively. This model is a simple expansion of the logistic model, with maximum rate of population growth given as $r_{max} = b_{max} - d_{min}$ and a carrying capacity defined as $K = \frac{b_{max} - d_{min}}{b_s + d_s}$. We redefine the logistic model this way to allow us to simulate the ecological dynamics as a stochastic birth-death process rather than a process with a net rate of population growth (Doebeli *et al.* 2017). We chose a

logistic-type model as an approximation of the sigmoidal population growth dynamics shown by a variety of organisms in relatively simple scenarios (Gause 1934; Sibly *et al.* 2005; Lee *et al.* 2018).

We consider the case where the maximum birth rate (b_{max}) is evolving and is connected to the minimum mortality through a classic life history trade-off between reproduction and mortality (i.e., the minimum death rate d_{min} is a function of b_{max}) (Stearns 1976; Reznick *et al.* 2000). This trade-off has been widely demonstrated across plants, invertebrates, and vertebrates (Lee *et al.* 2008; Wilder *et al.* 2013; Hosking *et al.* 2019). More practically, positing such a trade-off facilitates our analysis because it leads to an evolutionary equilibrium where fitness (here, the per-capita rate of population growth) is maximized. Using the QG approach, the dynamics of the population mean trait, $\overline{b_{max}}$, are given by

$$\frac{d\overline{b_{max}}}{dt} = V\left(\frac{\partial W}{\partial b_{max}}\right)_{b_{max}=\overline{b_{max}}},$$

where V is the product of narrow-sense heritability and additive genetic variance in b_{max}, $W = \frac{1}{R}\left(\frac{dR}{dt}\right)$ is the per-capita growth rate (i.e., mean individual fitness), and $\left(\frac{\partial W}{\partial b_{max}}\right)_{b_{max}=\overline{b_{max}}}$ is the fitness gradient evaluated at the mean trait. The fitness gradient will equal zero at the evolutionary equilibrium. Given equation (1) above, the fitness gradient is equal to $1 - d'_{min}\left(\overline{b_{max}}\right)$, which implies that the minimum death rate (d_{min}) must be an increasing function of the maximum birth rate (b_{max}) for an evolutionary equilibrium to exist (otherwise the fitness gradient will not change sign). For any equilibrium to represent a fitness maximum requires $\frac{\partial^2 W}{\partial b_{max}^2} = -d''_{min}(b_{max}) < 0$, which implies that the minimum death rate (d_{min}) must be an accelerating function of maximum birth rate (b_{max}). As such, we assume that $d_{min} = cb_{max}^2$, where c is a trade-off constant, making the equation for the evolutionary dynamics

$$\frac{d\overline{b_{max}}}{dt} = V\left(1 - 2c\overline{b_{max}}\right) \qquad \text{(Equation 2)}$$

Thus, in the deterministic QG model given by equations (1-2), the population will approach the eco-evolutionary equilibrium:

$$\left(\hat{R} = K = \frac{\overline{b_{max}} - \overline{d_{min}}}{b_s + d_s}, \overline{b_{max}} = \frac{1}{2c}\right). \quad \text{(Equation 3)}$$

We borrow the terminology of the adaptive dynamics literature and call this value of the mean maximum birth rate ($\overline{b_{max}}$) an evolutionarily stable strategy (ESS), since it is an evolutionary equilibrium where other trait values could not invade (in this case it is also the location where fitness is maximized).

Stochastic eco-evolutionary dynamics: GEMs simulate ecological dynamics through a stochastic birth-death process (DeLong & Gibert 2016; DeLong & Luhring 2018; DeLong & Belmaker 2019). GEMs build on the standard Gillespie algorithm for simulating ODE models where demographic stochasticity (random variation in the sequence and number of demographic events) influences population outcomes (Gillespie 1977; Yaari *et al.* 2012) and by incorporating demographic heterogeneity (variation among individuals in expected demographic traits) into the population. Unlike with a standard Gillespie algorithm, where population size is represented by a number, in a GEM, populations are represented as a collection of individuals with distinct trait values (i.e., parameters of the ecological model). Upon initiation of the simulation, the traits of these individuals are drawn from a probability distribution with a pre-defined mean and variance, with the type of distribution depending on the nature of the trait. Here, the trait of interest is maximum birth rate (b_{max}), which also determines the minimum death rate (d_{min}) through the trade-off function. Since b_{max} can only take positive values, we draw the b_{max} values for the initial population from a lognormal distribution.

In a GEM, an individual's trait value determines its probability of giving birth or dying. At each time step, an individual is chosen at random and its probability of birth or death is calculated by dividing the respective rate term by the sum of all rate terms. Noting that events generally do not have the same probability of occurrence, which event occurs is determined by a random draw from a uniform distribution (e.g., if the probability of birth is 0.4 and the probability of death is 0.6, the individual gives birth if the random draw is between 0 and 0.4 and dies otherwise). If the event is a death, that individual (really its trait) is removed from the population. If the event is a birth, a new individual is added to the

178 population, and its trait (b_{max}) is drawn from a lognormal distribution with a mean and variance that are
179 determined by the parental trait and specified rules for heritability of that trait (Appendix S1). As a GEM
180 is running, the loss and addition of individuals in the population affects both population dynamics and
181 the dynamics of both the mean and variance of the trait distribution(s). Populations gradually lose
182 individuals with high likelihood of mortality and gradually add individuals with higher likelihood of
183 births, generating natural selection without needing to specify fitness gradients, explicit equations for
184 the trait dynamics, or the expected trait equilibria such as an ESS. Evolutionary dynamics thus emerge
185 out of the stochastic births and deaths of individuals within the population (Dieckmann & Law 1996;
186 Champagnat *et al.* 2006; Doebeli *et al.* 2017), even as they are built on the deterministic equations that
187 can be used to formulate QG and AD approaches.
188 *Sets of comparisons:* We ran three sets of simulations, each with a specific purpose:
189 *The effect of individual variation on population abundance*.—We first examined the role of
190 individual variation in b_{max} and/or d_{min} on the ecological dynamics of this model when no evolution was
191 possible. To do this, we set heritability $h^2 = 0$ so that the parent's trait would not affect the trait of its
192 offspring. We set the initial population mean birth rate equal to $\overline{b_{max}} = 1.8$ and assumed a constant
193 trade-off parameter of $c = 0.0926$, which implies that the initial mean death rate was $\overline{d_{min}} = c\overline{b_{max}}^2 =$
194 $0.0926 \times 1.8^2 = 0.3$. We examined whether variation in neither trait, b_{max} alone, d_{min} alone, or both
195 traits combined influenced the dynamics. Since variation in d_{min} is normally linked to variation in b_{max} via
196 the trade-off function, we had to break the trade-off to evaluate the effect of variation in each
197 parameter on ecological dynamics separately. We first eliminated variation altogether by fixing both b_{max}
198 and d_{min} at their mean initial values (so all individuals had $b_{max} = 1.8$ and $d_{min} = 0.3$). Second, we
199 allowed variation in b_{max} around the initial value but fixed d_{min} at its initial value (so each individual had
200 b_{max} drawn from a lognormal distribution with a mean of 1.8 and a CV of 0.3 and $d_{min} = 0.3$). Third, we
201 generated variation in d_{min} by first allowing variation in b_{max} to drive variation in d_{min} according to our

trade-off, but we then re-set all b_{max} values for individuals to the mean value (so each individual had $b_{max} = 1.8$ and d_{min} equal to the trade-off parameter *c* multiplied by the square of a value drawn from a lognormal distribution with a mean of 1.8 and a CV of 0.3). This also removes the trade-off between b_{max} and d_{min}. This examination also confirmed that the GEM dynamics reduced to a standard Gillespie simulation of the ecological model at larger population sizes (Equation 1). We used carrying capacities of 10 and 40, created by setting $b_s = d_s = 0.075$ and 0.0187, respectively (and assuming $\overline{b_{max}} = 1.8$ and $\overline{d_{min}} = 0.3$ [Eq. 3]). We initialized populations with five individuals and ran each simulation for 30 time steps and replicated each stochastic simulation 200 times.

The effect of demographic stochasticity on evolutionary outcomes.—We next evaluated differences between the GEM and QG approaches by comparing outcomes across three different levels of density dependence. We set the initial carrying capacity (*K*) at 10, 20, and 40, created by setting $b_s = d_s = 0.075$, 0.0375, and 0.0187, respectively; note that as the populations evolve and $\overline{b_{max}}$ changes, the carrying capacity changes as well [Eq. 3]. We initialized populations with five individuals using the same initial trait values as above. The ESS $\overline{b_{max}}$ for this system is 5.4, which means the ESS $\overline{d_{min}}$ is 2.7. The CV of the evolving trait (maximum birth rate, b_{max}) in the initial population was 0.3, such that the mean initial variance in b_{max} was about 0.29 (due to stochastic sampling), and heritability (h^2) was 0.75. For a check on the effect of the trade-off parameter, we also varied *c* (0.06, 0.09, and 1.2), using the same trait values and one level of density dependence ($b_s = d_s = 0.04$). We expected that populations with smaller carrying capacity would demonstrate greater stochasticity and average abundances farther below their carrying capacity than in the populations with larger carrying capacity, generating a more pronounced effect of transient behavior on the evolving trait. We expected higher carrying capacity would facilitate convergence of the GEM solution with the QG solution. We ran each simulation for 400 time steps and replicated each stochastic simulation 50 times.

To evaluate patterns in individual fitness (here, lifetime reproductive success) across GEM simulations, we tracked the number of reproductive events and the lifespan for each individual. This allowed us to visualize the realized relationship between each individual's maximum birth rate (b_{max}) and lifetime reproductive success, akin to Figure 1B. We do this for the population toward the end of the simulation (born after time step 350), including only individuals that died before the end of the simulation.

The effect of culling on evolutionary outcomes.—We next asked how culling a population that has already achieved an eco-evolutionary equilibrium would cause the population to evolve when the probability of death due to the cull was independent of an individual's traits. The deterministic model for the population dynamics for the birth-death logistic model with an additional culling term is the following:

$$\frac{dR}{dt} = (b_{max} - b_s R)R - (d_{min} + d_s R)R - x \max(0, R - R_{cull}).$$

Under this model, we cull the population at the rate x whenever $R > R_{cull}$. As $x \to \infty$, the equilibrium $\hat{R} \to R_{cull}$. As we show in Appendix S2, because this culling is trait-independent, the evolutionary dynamics for the mean trait $\left(d\overline{b_{max}}/dt\right)$ are still given by equation (2) above. We do this with an intermediate level of density dependence with three levels of culling. We used the same trait scheme as above, but we initialized populations with 72 individuals with $\overline{b_{max}} = 5.4$ (thus at the eco-evolutionary equilibrium for $b_s = d_s = 0.0187$). Individuals were culled at random with respect to their traits with a culling rate of $x = 10{,}000$ (which ensures that the population size rapidly approaches R_{cull}) and R_{cull} values of 50, 30, or 10. We ran each simulation for 400 time steps and replicated each stochastic simulation 50 times. We also tracked lifetime reproductive success in this set of simulations.

Results

The effect of individual variation on population abundance.—In the first comparison, we sought to determine if individual variation and stochasticity altered population abundance relative to the expected

equilibrium abundance. Reducing heritability to zero effectively eliminates evolution by natural selection, revealing how stochasticity and trait variation *per se* alters the dynamics of the system (Figure 2). At low carrying capacity (K = 10) and without trait variation, average population size remained below carrying capacity and showed considerable variation (Figure 2A), but the average population size was much closer to carrying capacity and less variable when K = 40 (Figure 2E), indicating that demographic stochasticity lowers average abundance and does so more when there is more stochasticity. Adding variation in either the maximum birth rate (b_{max}) or minimum death rate (d_{min}) alone, or combination, had the effect of lowering average population abundance compared to the expectation at both low K (Figure 2B-D) and high K (Figure 2F-H). This result indicates that both stochasticity and trait variation *per se* may generate average abundances that are relatively steady but persistently below equilibrium, an effect that is often amplified if the varying traits are involved in trade-off (Nisbet & Gurney 1982; Stover *et al.* 2012b; Cressler *et al.* 2017). Thus, the dynamics exhibit a type of long transient (Hastings *et al.* 2018).

The effect of demographic stochasticity on evolutionary outcomes.—In our second set of simulations, we sought to determine whether the stochasticity generated by low population size and the resultant below-expected average abundances altered evolutionary outcomes. In this comparison, we varied only the strength of density dependence, and we found that all populations grew towards the expected ecological equilibrium and b_{max} evolved towards the ESS (Figure 3, 1st, 2nd, and 5th rows). Although no population was able to grow or evolve as fast as expected from QG (Figure 3, 1st and 2nd rows), the population experiencing the least density dependence converged to the expected eco-evolutionary equilibrium while the populations with higher density dependence lagged behind. The depiction of the eco-evolutionary dynamics in the phase plane (Fig. 3, row 5) is also illustrative: the initial ecological dynamics are much faster than the evolutionary dynamics (the initial movement in the phase plane is

mostly in the direction of increasing population abundance), and then both abundance and the trait increase together towards the eco-evolutionary equilibrium given by the orange point (Fig. 3, 5th row).

We also found that populations with stronger density dependence (i.e., higher values of b_s and d_s and therefore lower K_{init} values) experienced greater initial loss of trait variation (Figure 3, 3rd row). This loss of variation slows the pace of evolution relative to the QG expectation. At intermediate and low density dependence (higher K_{init}), the initial loss of trait variation was more temporary, allowing populations to recover from the effects of low-density stochasticity and continue moving in the direction of the ESS. As expected, the effects of stochasticity were noticeably higher for small populations, with considerably more variation in abundances through time for populations with the highest density dependence (Figure 3, left column). However, all populations displayed considerable individual demographic stochasticity (Figure 3, 4th row), manifested as large differences in lifetime reproductive success among individuals with the same trait values. In addition, there was considerable demographic heterogeneity in the populations even after the distribution of maximum birth rate (b_{max}) values had centered on the optimal (ESS) values.

It is also clear that the evolutionary dynamics often do not reach the expected evolutionary equilibrium, especially in small populations where demographic stochasticity is strong. In particular, the median of the stochastic trajectories often settles onto or approaches a trait value that is noticeably smaller than the ESS (Fig. 3 row 2 and 5). To help understand this result, we calculated the expected lifetime reproductive success (LRS) of an individual from the model:

$$\mathrm{LRS} = \frac{(b_{max} - b_s R)}{(d_{min} + d_s R)}. \qquad \text{(Equation 4)}$$

The value of maximum birth rate (b_{max}) that maximizes LRS is given by the solution of the equation $\frac{\partial \mathrm{LRS}}{\partial b_{max}} = 0$:

$$b_{max} = b_s R + \sqrt{(b_s R)^2 + \frac{d_s R}{c}}. \qquad \text{(Equation 5)}$$

Our motivation for calculating LRS is two-fold. First, we can calculate an expected LRS for an individual, but we can also compare that expectation to the stochastically realized LRS in our GEM simulation. Second, classic theory and its more modern incarnations suggest that evolution maximizes LRS when populations are at equilibrium, whereas it maximizes per-capita growth rate in growing populations (MacArthur 1962; MacArthur & Wilson 2001; Lande *et al.* 2009; Engen & Sæther 2017). Note that the value of b_{max} that maximizes expected lifetime reproductive success is not necessarily the same as the ESS value (although when R is at its deterministic equilibrium, the values are the same). In particular, this value depends on the current population size, meaning that the value of b_{max} that maximizes lifetime reproductive success changes as the population grows. We term this transient peak on the fitness landscape a "transient evolutionary attractor" (TEA), because it both attracts the population and changes as the population moves through its transient dynamics. Re-examining the observed lifetime reproductive success values, it is clear that the peak of the observed distribution is often centered on these TEAs (Fig. 3, 4th row), and that the observed evolutionary trajectory for b_{max} often appears to be approaching this TEA rather than the ESS (Fig. 3, 2nd and 5th rows). The outcome in which populations evolved toward a TEA rather than an ESS holds across a range of values for the trade-off slope, c (Figure S5).

The effect of culling on evolutionary outcomes.—In our third set of simulations, we sought to understand whether an external force altering population size would drive evolution away from the expected ESS, given the dependence of the optimal trait value on abundance. Here we applied a persistent cull to populations that had already achieved their ESS trait and abundance values. Because we assumed a large value for the culling rate x, the population size changed almost immediately so that $R \approx R_{cull}$. This change in population size led to a clear evolutionary trajectory of the maximum birth rate (b_{max}) away from the ESS. Again, we can ask what value of b_{max} maximizes expected reproductive success. The expected lifetime reproductive success under culling is

$$\mathrm{LRS} = \frac{b_{max} - b_s R}{d_{min} + d_s R + x \max\left(0, 1 - \frac{R_{cull}}{R}\right)}. \qquad \text{(Equation 6)}$$

Assuming that $R \approx R_{cull}$, the value of b_{max} that maximizes LRS is again given by Eq. (5) above. Fig. 4 shows clearly that the population mean b_{max} evolved to the population-specific TEAs that depended on the population size the cull produced (seen by the intersection of the population with the black line; Figure 4, bottom row). Rather than returning to the ESS, populations that were culled to a lower abundance evolved toward the optimal trait (i.e., showing the highest lifetime reproductive success) for that culled abundance (i.e., the TEA) and away from the ESS (Figure 4). The populations followed a path of adaptation specific to the current transient state, as generated by Equation 5, not the path generated by equilibrium conditions and suggested by QG.

Discussion

Evolutionary theory today encompasses a wide range of modeling techniques and frameworks that facilitate an understanding of how populations evolve and adapt to their environments (Lande 1982; Abrams *et al.* 1993a; DeAngelis & Mooij 2005; Coulson *et al.* 2006; Ellner & Rees 2006; Lion 2017; de Vries & Caswell 2019; Govaert *et al.* 2019). Doebeli *et al.* (2017) has argued that the mechanistic foundation for evolutionary theory should be stochastic birth-death processes. However, while such models can readily be simulated, as we do here, deterministic approximations of such stochastic processes are required to make limiting assumptions, such as a separation of ecological and evolutionary timescales, weak selection, small mutational effects, or large population size (Dieckmann & Law 1996; Champagnat *et al.* 2006; Doebeli *et al.* 2017; Parsons *et al.* 2018). Here we show two important results. First, when populations are large, the deterministic approximations can provide an accurate description of both the transient and equilibrium behavior of the ecological and evolutionary dynamics (Fig. 3, right column). This is expected, since the assumption of large population sizes is included in most classic evolutionary theory, but is still reassuring. Second, even when these limiting assumptions are not met and the stochastic eco-evolutionary dynamics do not exactly match the

deterministic expectation, the deterministic equations can still be useful in helping to understand the resulting eco-evolutionary dynamics. In particular, we show that demographic heterogeneity (trait variance) and demographic stochasticity can keep populations away from an expected ecological equilibrium (and therefore in a transient state), and that under such conditions the population mean traits can evolve towards transient evolutionary attractors (TEAs) that maximize LRS, rather than the ESS. The eco-evolutionary dynamics and the pace and path of evolution, then, are qualitatively and quantitatively different from predictions that overlook transient periods of evolution, such as classic adaptive dynamics approaches that assume a separation of ecological and evolutionary timescales (Geritz *et al.* 1998; Abrams 2001). The transient evolutionary dynamics that unfolded during our GEM simulations here responded to underlying fitness gradients that are invisible with an equilibrium lens but that lay out a straightforward evolutionary path that transient populations can follow. With the rapid environmental change and direct human impact that disrupts populations throughout the world today, these results suggest that theories of evolution that focus on stochastic birth-death processes, and the transient, non-equilibrium dynamics of such processes, will provide crucial new insights into adaptation.

The mechanisms generating our results are two-fold. First, demographic stochasticity and demographic heterogeneity (individual variation in traits) combine to suppress population growth below its deterministic, homogeneous expectation. Our non-evolutionary simulations without trait variance show that smaller populations will have greater variability and average farther below the expected equilibrium than larger populations (Figure 1) due to demographic stochasticity, a classic and unsurprising result (Nisbet & Gurney 1982). Adding trait variation to the populations further lowers average abundance, reinforcing the transient state of the populations (Stover *et al.* 2012b; Cressler *et al.* 2017). Second, although the population size never truly reaches an equilibrium, it does reach an approximately steady state where population growth rate is nearly zero. Under this scenario, evolution tends to maximize lifetime reproductive success rather than per-capita growth rate (MacArthur 1962;

MacArthur & Wilson 2001; Lande *et al.* 2009; Engen & Sæther 2017). The intuition for this prediction is straightforward: if population size is changing, then having offspring more quickly is important, and per-capita growth rate is the appropriate measure of fitness; if population size is (relatively) constant, then the timing of reproduction matters less than the total amount of reproduction, and lifetime reproductive success is a more appropriate measure of fitness. Together, these mechanisms can limit the approach of a population to its equilibrium and thus relocate the fitness peak and redirect evolution to an unexpected location, a transient evolutionary attractor (TEA). Our culling simulations indicate that external forces can also cause this effect if the culling is independent of the traits (Figure 4).

In addition to the effects caused by the TEAs, our results indicate that the presence of individual trait variation (and the resulting demographic heterogeneity; Kendall *et al.* 2011; Stover *et al.* 2012), although required for evolution to proceed, can itself change the ecological dynamics. In our case, this variation simultaneously facilitated evolution by providing raw material upon which selection could act and maintained the system in a transient state (i.e., a state in which the ecological equilibrium has not been attained) such that the expected evolutionary equilibrium could not be attained. Individual demographic stochasticity, abundantly displayed in our results, clearly influenced the relationship between fitness and traits, causing some individuals with traits that would be expected to lead to low lifetime reproductive success to actually realize high fitness, while some individuals with high fitness traits to realize low fitness (Figures 3 and 5, 4^{th} row). This effect should result in a flattened fitness gradient relative to the expectations from quantitative genetics, greatly reducing the rate of evolution and maintaining individual variation (Cressler *et al.* 2017). Finally, demographic stochasticity generated heightened variation in population size for small populations, both keeping populations in transient states and leading to substantial initial loss of genetic variation. Examination of the population dynamics in the systems with lower carrying capacities (Figure 3, left column) indicates more variation in

population sizes, reflecting high stochasticity. All together, these forces substantially slowed evolution relative to expectations generated from classic assumptions of deterministic evolutionary theory.

Increasing evidence indicates that ecological dynamics can play a crucial role in shaping evolution (Pimentel 1961; Grant & Grant 2002; Yoshida *et al.* 2004; Hairston *et al.* 2005; Schoener 2011; Lowe *et al.* 2017). Furthermore, evolution within systems not at equilibrium, and rather displaying transient dynamics (Hastings *et al.* 2018), can alter the ecological dynamics and therefore the selective forces acting on the population (Fussmann *et al.* 2003; Yoshida *et al.* 2003; Cortez & Weitz 2014; Lowe *et al.* 2017). Our results further this finding, demonstrating that even simple, single-species models can facilitate not just eco-evolutionary dynamics but generate transient evolutionary attractors (TEAs) that may compete with the overall evolutionary attractor in the system (the ESS). By taking into account the full consequences of individual variation and stochasticity, we may generate more realistic predictions for evolution. We do not, however, suggest that TEAs will be present in all systems. The minimum requirement for a TEA is that the expression $\frac{\partial \text{fitness}}{\partial \text{trait}} = 0$ must actually have a solution, otherwise there is neither an ESS nor a TEA. Furthermore, if there is density dependence in birth or death rates, then the trait value that maximizes lifetime reproductive success will always be a function of density. Therefore, this maximum will not be the same away from equilibrium (the TEA) as it is at equilibrium (the ESS). In our Equation 5, a lifetime reproductive success maximum exists and population abundance *R* is present in the expression, generating a TEA. Thus, to the extent that these conditions are met, likely in most cases of density-dependent demographics with some sort of trade-off among fitness related traits, TEAs may be a common feature of evolutionary pathways.

One of the most non-intuitive results here is that culling can dramatically alter the evolutionary dynamics from the expectation. As we show in Appendix S2, trait-independent culling does not alter the expected evolutionary dynamics based on quantitative genetics, and thus we would expect that a population whose trait was already at the ESS would not evolve away from it. And yet, we see that trait

evolution moves away from the ESS and towards the TEA (Fig. 5) when the population is culled. As a consequence, our results may have important implications for managed populations. Economically important populations, from fisheries to ungulates and invasive species, may show substantial changes in traits in response to random or trait-biased harvesting (Darimont *et al.* 2009). In Windermere pike (*Esox lucius*), for example, harvesting is thought to have altered the fitness landscape and generated selection away from the direction driven by the natural setting (Edeline *et al.* 2007). This evolutionary outcome could represent both the direct selective effects of harvesting itself but also the presence of a transient attractor that competed with an ESS attractor, since harvesting maintained populations in a transient state. Understanding evolution in such populations may require a disequilibrium (transient) approach, because harvested populations are by definition being held below their potential equilibrium. To the degree that these populations show density dependence in their birth or death rates, similar to but not necessarily following the birth-death logistic model, they are likely to also display TEAs that could draw their traits away from the starting values, whether the initial trait distributions are at the ESS value or not. Culling our simulated population nearly halved the fecundity of the population, even without it having a direct selective effect (as captured by the equation for the evolutionary dynamics). This would have long-term ramifications for the culled population, as the ecological equilibrium would not quickly return to the pre-cull levels upon relaxation of the cull.

Studying the evolutionary process from the perspective of stochastic birth-death processes increases the opportunity for profitable cross-pollination between ecological and evolutionary theory (Doebeli *et al.* 2017). In particular, while other authors have used approaches very similar to GEMs to test the predictions of classic evolutionary theory (e.g., Claessen *et al.* 2007), GEMs provide a natural and straightforward way to reformulate classic ecological models into stochastic evolutionary birth-death processes (DeLong & Gibert 2016; DeLong & Luhring 2018; DeLong & Belmaker 2019), allowing

ecologists and evolutionary biologists to study the feedback between ecological and evolutionary dynamics that emerges out of such a reformulation.

In conclusion, our results indicate that stochastic birth-death processes, by introducing individual variation and demographic stochasticity, can produce evolutionary trajectories that differ significantly from expectations based on deterministic approaches, revealing powerful competing evolutionary attractors (TEAs) that have not factored into much (if any) current thinking about the pace and path of adaptation. However, we also find that these TEAs can still be understood via the deterministic approximations, helping to reveal both the utility and the limitations of such approximations. Becoming aware that evolution is relatively fast, and that many populations are in transient states rather than equilibrium states, may be essential for a fuller understanding of adaptation.

Acknowledgements

This work was supported in part by a grant to JPD from James S. McDonnell Foundation Studying Complex Systems Scholar Award. The authors thank Troy Day for helpful feedback on an early version of this manuscript, and the associate editor and two reviewers for comments and suggestions that greatly improved this manuscript.

References

Abbott, K.C. & Nolting, B.C. (2017). Alternative (un)stable states in a stochastic predator–prey model. *Ecological Complexity*, Uncertainty in Ecology, 32, 181–195.

Abrams. (2001). Modelling the adaptive dynamics of traits involved in inter- and intraspecific interactions: An assessment of three methods. *Ecology Letters*, 4, 166–175.

Abrams, P.A., Harada, Y. & Matsuda, H. (1993a). On the relationship between quantitative genetic and ESS models. *Evolution*, 47, 982–985.

Abrams, P.A., Matsuda, H. & Harada, Y. (1993b). Evolutionarily unstable fitness maxima and stable fitness minima of continuous traits. *Evol Ecol*, 7, 465–487.

Abrams, P.A., Matsuda, H. & Harada, Y. (1993c). Evolutionarily unstable fitness maxima and stable fitness minima of continuous traits. *Evol Ecol*, 7, 465–487.

Andrewartha, H.G. & Birch, L.C. (1954). *The distribution and abundance of animals*. University of Chicago Press.

Ashwin, P., Wieczorek, S., Vitolo, R. & Cox, P. (2012). Tipping points in open systems: bifurcation, noise-induced and rate-dependent examples in the climate system. *Philosophical Transactions of the Royal Society A: Mathematical, Physical and Engineering Sciences*, 370, 1166–1184.

Banks, M.J. & Thompson, D.J. (1987). Lifetime reproductive success of females of the damselfly *Coenagrion puella*. *Journal of Animal Ecology*, 56, 815–832.

Black, A.J. & McKane, A.J. (2012). Stochastic formulation of ecological models and their applications. *Trends Ecol. Evol. (Amst.)*, 27, 337–345.

Bolnick, D.I., Amarasekare, P., Araújo, M.S., Bürger, R., Levine, J.M., Novak, M., *et al.* (2011). Why intraspecific trait variation matters in community ecology. *Trends Ecol. Evol.*, 26, 183–192.

Champagnat, N., Ferrière, R. & Méléard, S. (2006). Unifying evolutionary dynamics: from individual stochastic processes to macroscopic models. *Theor Popul Biol*, 69, 297–321.

Childs, D.Z., Metcalf, C.J.E. & Rees, M. (2010). Evolutionary bet-hedging in the real world: empirical evidence and challenges revealed by plants. *Proc. Biol. Sci.*, 277, 3055–3064.

Claessen, D., Andersson, J., Persson, L. & de Roos, A.M. (2007). Delayed evolutionary branching in small populations. *Evolutionary Ecology Research*, 9, 51–69.

Cohen, D. (1966). Optimizing reproduction in a randomly varying environment. *Journal of Theoretical Biology*, 12, 119–129.

Cortez, M.H. (2016). How the magnitude of prey genetic variation alters predator-prey eco-evolutionary dynamics. *The American Naturalist*, 188, 329–341.

Cortez, M.H. & Ellner, S.P. (2010). Understanding rapid evolution in predator-prey interactions using the theory of fast-slow dynamical systems. *Am. Nat.*, 176, E109-127.

Cortez, M.H. & Weitz, J.S. (2014). Coevolution can reverse predator–prey cycles. *Proc Natl Acad Sci U S A*, 111, 7486–7491.

Coulson, T., Benton, T.G., Lundberg, P., Dall, S.R.X. & Kendall, B.E. (2006). Putting evolutionary biology back in the ecological theatre: a demographic framework mapping genes to communities. *Evol Ecol Res*, 8, 1155–1171.

Coulson, T., Rohani, P. & Pascual, M. (2004). Skeletons, noise and population growth: the end of an old debate? *Trends Ecol. Evol. (Amst.)*, 19, 359–364.

Coyne, J.A., Barton, N.H. & Turelli, M. (1997). Perspective: A Critique of Sewall Wright's Shifting Balance Theory of Evolution. *Evolution*, 51, 643–671.

Crespi, B.J. (2000). The evolution of maladaptation. *Heredity (Edinb)*, 84 (Pt 6), 623–629.

Cressler, C.E., Bengtson, S. & Nelson, W.A. (2017). Unexpected nongenetic individual heterogeneity and trait covariance in *Daphnia* and its consequences for ecological and evolutionary dynamics. *The American Naturalist*, 190, E13–E27.

van Daalen, S.F. & Caswell, H. (2017). Lifetime reproductive output: individual stochasticity, variance, and sensitivity analysis. *Theor Ecol*, 10, 355–374.

Darimont, C.T., Carlson, S.M., Kinnison, M.T., Paquet, P.C., Reimchen, T.E. & Wilmers, C.C. (2009). Human predators outpace other agents of trait change in the wild. *PNAS*, 106, 952–954.

Day, T. & Gandon, S. (2006). Insights from Price's equation into evolutionary epidemiology. *Disease evolution: models, concepts, and data analyses*, 71, 23.

DeAngelis, D.L. & Mooij, W.M. (2005). Individual-based modeling of ecological and evolutionary processes. *Annual Review of Ecology, Evolution, and Systematics*, 36, 147–168.

DeLong, J.P. & Belmaker, J. (2019). Ecological pleiotropy and indirect effects alter the potential for evolutionary rescue. *Evolutionary Applications*, 12, 636–654.

DeLong, J.P. & Gibert, J.P. (2016). Gillespie eco-evolutionary models (GEMs) reveal the role of heritable trait variation in eco-evolutionary dynamics. *Ecol Evol*, 6, 935–945.

DeLong, J.P. & Luhring, T.M. (2018). Size-dependent predation and correlated life history traits alter eco-evolutionary dynamics and selection for faster individual growth. *Popul Ecol*, 60, 9–20.

Dieckmann, U. & Law, R. (1996). The dynamical theory of coevolution: a derivation from stochastic ecological processes. *J Math Biol*, 34, 579–612.

Doebeli, M., Ispolatov, Y. & Simon, B. (2017). Towards a mechanistic foundation of evolutionary theory. *eLife*, 6, e23804.

Edeline, E., Carlson, S.M., Stige, L.C., Winfield, I.J., Fletcher, J.M., James, J.B., *et al.* (2007). Trait changes in a harvested population are driven by a dynamic tug-of-war between natural and harvest selection. *PNAS*, 104, 15799–15804.

Ellner, S.P. & Rees, M. (2006). Integral projection models for species with complex demography. *Am. Nat.*, 167, 410–428.

Engen, S. & Sæther, B.-E. (2017). r- and K-selection in fluctuating populations is determined by the evolutionary trade-off between two fitness measures: Growth rate and lifetime reproductive success. *Evolution*, 71, 167–173.

Fisher, R.A. (1930). *The Genetical Theory of Natural Selection: A Complete Variorum Edition*. OUP Oxford.

Fussmann, G.F., Ellner, S.P. & Hairston, N.G., Jr. (2003). Evolution as a critical component of plankton dynamics. *Proc. Biol. Sci.*, 270, 1015–1022.

Gause, G.F. (1934). *The Struggle for Existence.* Williams and Wilkins, Baltimore (Reprinted 1964 by Hafner).

Geritz, S.A.H., Kisdi, E., Mesze´NA, G. & Metz, J.A.J. (1998). Evolutionarily singular strategies and the adaptive growth and branching of the evolutionary tree. *Evolutionary Ecology*, 12, 35–57.

Gillespie, D.T. (1977). Exact stochastic simulation of coupled chemical reactions. *J. Phys. Chem.*, 81, 2340–2361.

Govaert, L., Fronhofer, E.A., Lion, S., Eizaguirre, C., Bonte, D., Egas, M., *et al.* (2019). Eco-evolutionary feedbacks—Theoretical models and perspectives. *Functional Ecology*, 33, 13–30.

Grant, P.R. & Grant, B.R. (2002). Unpredictable evolution in a 30-Year study of Darwin's finches. *Science*, 296, 707–711.

Greenman, J.V. & Benton, T.G. (2003). The amplification of environmental noise in population models: causes and consequences. *Am. Nat.*, 161, 225–239.

Hairston, Jr., N.G., Ellner, S.P., Geber, M.A., Yoshida, T. & Fox, J.A. (2005). Rapid evolution and the convergence of ecological and evolutionary time. *Ecol. Lett.*, 8, 1114–1127.

Hastings, A., Abbott, K.C., Cuddington, K., Francis, T., Gellner, G., Lai, Y.-C., *et al.* (2018). Transient phenomena in ecology. *Science*, 361.

552 Henson, S.M., Cushing, J.M., Costantino, R.F., Dennis, B. & Desharnais, R.A. (1998). Phase
553 switching in population cycles. *Proceedings of the Royal Society of London. Series B:*
554 *Biological Sciences*, 265, 2229–2234.
555 Hosking, C.J., Raubenheimer, D., Charleston, M.A., Simpson, S.J. & Senior, A.M. (2019).
556 Macronutrient intakes and the lifespan-fecundity trade-off: a geometric framework
557 agent-based model. *Journal of The Royal Society Interface*, 16, 20180733.
558 Humplik, J., Hill, A.L. & Nowak, M.A. (2014). Evolutionary dynamics of infectious diseases in
559 finite populations. *J. Theor. Biol.*, 360, 149–162.
560 Ives, A.R., Einarsson, A., Jansen, V.A.A. & Gardarsson, A. (2008). High-amplitude fluctuations
561 and alternative dynamical states of midges in Lake Myvatn. *Nature*, 452, 84–87.
562 Iwasa, Y., Pomiankowski, A. & Nee, S. (1991). The evolution of costly mate preferences Ii. the
563 "handicap" principle. *Evolution*, 45, 1431–1442.
564 Kendall, B.E., Fox, G.A., Fujiwara, M. & Nogeire, T.M. (2011). Demographic heterogeneity,
565 cohort selection, and population growth. *Ecology*, 92, 1985–1993.
566 Lande, R. (1976). Natural selection and random genetic drift in phenotypic evolution. *Evolution*,
567 30, 314–334.
568 Lande, R. (1982). A quantitative genetic theory of Life history evolution. *Ecology*, 63, 607–615.
569 Lande, R., Engen, S. & Sæther, B.-E. (2009). An evolutionary maximum principle for density-
570 dependent population dynamics in a fluctuating environment. *Philosophical*
571 *Transactions of the Royal Society B: Biological Sciences*, 364, 1511–1518.
572 Lee, D.E., Berger, R.W., Tietz, J.R., Warzybok, P., Bradley, R.W., Orr, A.J., *et al.* (2018). Initial
573 growth of northern fur seal (*Callorhinus ursinus*) colonies at the South Farallon, San
574 Miguel, and Bogoslof Islands. *J Mammal*, 99, 1529–1538.
575 Lee, K.P., Simpson, S.J., Clissold, F.J., Brooks, R., Ballard, J.W.O., Taylor, P.W., *et al.* (2008).
576 Lifespan and reproduction in Drosophila: New insights from nutritional geometry. *Proc*
577 *Natl Acad Sci U S A*, 105, 2498–2503.
578 Lenormand, T., Roze, D. & Rousset, F. (2009). Stochasticity in evolution. *Trends in Ecology &*
579 *Evolution*, 24, 157–165.
580 Lion, S. (2017). Theoretical approaches in evolutionary ecology: Environmental feedback as a
581 unifying perspective. *The American Naturalist*, 191, 21–44.
582 Lowe, W.H., Kovach, R.P. & Allendorf, F.W. (2017). Population genetics and demography unite
583 ecology and evolution. *Trends Ecol. Evol. (Amst.)*, 32, 141–152.
584 MacArthur, R.H. (1962). Some Generalized Theorems of Natural Selection. *PNAS*, 48, 1893–
585 1897.
586 MacArthur, R.H. & Wilson, E.O. (2001). *The Theory of Island Biogeography*. Princeton University
587 Press.
588 McKane, A.J. & Newman, T.J. (2005). Predator-prey cycles from resonant amplification of
589 demographic stochasticity. *Phys. Rev. Lett.*, 94, 218102.
590 Nicholson, A.J. (1957). The self-adjustment of populations to change. *Cold Spring Harb Symp*
591 *Quant Biol*, 22, 153–173.
592 Nisbet, R.M. & Gurney, W.S.C. (1982). *Modelling Fluctuating Populations*. Wiley.
593 Parsons, T.L., Lambert, A., Day, T. & Gandon, S. (2018). Pathogen evolution in finite populations:
594 slow and steady spreads the best. *Journal of The Royal Society Interface*, 15, 20180135.

Pimentel, D. (1961). Animal population regulation by the genetic feed-back mechanism. *The American Naturalist*, 95, 65–79.
Proulx, S.R. & Day, T. (2001). What can invasion analyses tell us about evolution under stochasticity in finite populations? *Selection*, 2, 2–15.
Queller, D.C. (2017). Fundamental Theorems of Evolution. *Am. Nat.*, 189, 345–353.
Rees, M. & Ellner, S.P. (2019). Why so variable: Can genetic variance in flowering thresholds be maintained by fluctuating selection? *The American Naturalist*, 194, E13–E29.
Reznick, D., Nunney, L. & Tessier, A. (2000). Big houses, big cars, superfleas and the costs of reproduction. *Trends in Ecology & Evolution*, 15, 421–425.
Schoener, T.W. (2011). The newest synthesis: understanding the interplay of evolutionary and ecological dynamics. *Science*, 331, 426–429.
Sibly, R.M., Barker, D., Denham, M.C., Hone, J. & Pagel, M. (2005). On the regulation of populations of mammals, birds, fish, and insects. *Science*, 309, 607–610.
Start, D., Weis, A.E. & Gilbert, B. (2020). Ecological and evolutionary stochasticity shape natural selection. *The American Naturalist*, 195, 705–716.
Stearns, S.C. (1976). Life-History Tactics: A Review of the Ideas. *The Quarterly Review of Biology*, 51, 3–47.
Stover, J.P., Kendall, B.E. & Fox, G.A. (2012a). Demographic heterogeneity impacts density-dependent population dynamics. *Theor Ecol*, 5, 297–309.
Stover, J.P., Kendall, B.E. & Fox, G.A. (2012b). Demographic heterogeneity impacts density-dependent population dynamics. *Theor Ecol*, 5, 297–309.
Taper, M.L. & Case, T.J. (1992). Models of character displacement and the theoretical robustness of taxon cycles. *Evolution*, 46, 317–333.
Taylor, P. & Day, T. (1997). Evolutionary stability under the replicator and the gradient dynamics. *Evol Ecol*, 11, 579–590.
Tirok, K., Bauer, B., Wirtz, K. & Gaedke, U. (2011). Predator-prey dynamics driven by feedback between functionally diverse trophic levels. *PLoS ONE*, 6, e27357.
Vasseur, D.A., Amarasekare, P., Rudolf, V.H.W. & Levine, J.M. (2011). Eco-evolutionary dynamics enable coexistence via neighbor-dependent selection. *Am. Nat.*, 178, E96–E109.
de Vries, C. & Caswell, H. (2019). Stage-structured evolutionary demography: Linking life histories, population genetics, and ecological dynamics. *The American Naturalist*, 193, 545–559.
Wakano, J.Y. & Iwasa, Y. (2013). Evolutionary Branching in a Finite Population: Deterministic Branching vs. Stochastic Branching. *Genetics*, 193, 229–241.
Wilder, S.M., Le Couteur, D.G. & Simpson, S.J. (2013). Diet mediates the relationship between longevity and reproduction in mammals. *AGE*, 35, 921–927.
Wright, S. (1931). Evolution in Mendelian populations. *Genetics*, 16, 97–159.
Yaari, G., Ben-Zion, Y., Shnerb, N.M. & Vasseur, D.A. (2012). Consistent scaling of persistence time in metapopulations. *Ecology*, 93, 1214–1227.
Yoshida, T., Jones, L.E., Ellner, S.P., Fussmann, G.F. & Hairston, Jr., N.G. (2003). Rapid evolution drives ecological dynamics in a predator-prey system. *Nature*, 424, 303–306.

637 Yoshida, T., Jr, N.G.H. & Ellner, S.P. (2004). Evolutionary trade-off between defence against
638 grazing and competitive ability in a simple unicellular alga, Chlorella vulgaris. *Proc Biol*
639 *Sci.*, 271, 1947–1953.
640

Figure 1. Variation in the relationship between traits and fitness. A. A depiction of how stochasticity and heterogeneity map on to the relationship between traits and fitness. B. An example of this relationship with the damselfly *Coenagrion puella* (Banks & Thompson 1987). These data show that lifetime reproductive success (here lifetime clutches) may reach a peak at some intermediate trait value (near 4.1 mm; shading shows the general vicinity of the optimal trait). Simultaneously, individuals may vary dramatically in their realized fitness despite having similar traits.

Figure 2. Results of a non-evolutionary GEM simulation of the birth-death logistic model evaluating the effects of trait variation on the dynamics. In these simulations, heritability was set to zero, and variation was allowed in neither trait (A), in only maximum birth rate (b_{max}) (B), in only minimum death rate (d_{min}) (C), and in both d_{min} and b_{max} (D). In A, all trait variation was removed, causing the simulations to collapse on the non-evolutionary ordinary differential equation (ODE) solution (as generated by Equation 1). This indicates that the GEM effectively collapses to a standard Gillespie simulation in the absence of trait variance and heritability. In B, variation in mortality (d_{min}) was removed by setting it equal to the mean value for all individuals, but variation in b_{max} was retained (see main text). In C, we generated variation in d_{min} by calculating it for all individuals from their b_{max}, but then resetting b_{max} to the mean. In D, variation in both traits was retained. This final panel indicates that trait variation (demographic heterogeneity) alters the ecology of the system, lowering the abundance at equilibrium relative to that expected from the mean traits themselves. The median (dark solid line) and middle 50% (shaded area) of 50 simulations are shown.

Figure 3. Gillespie eco-evolutionary model (GEM) simulations of the birth-death logistic model. The rows show from top to bottom population abundance, mean maximum birth rate (b_{max}), variance in b_{max}, lifetime reproductive success (product of expected births and expected lifespan), and the mean

665 trajectory through the abundance-b_{max} phase plane. The columns show three levels of density
666 dependence in birth and death rates (values of b_s and d_s) that set the initial carrying capacity at 10, 20,
667 and 40 from left to right. (The initial carrying capacity is the ecological equilibrium if b_{max} remained fixed
668 at 1.8.) The median and middle 50% of 50 stochastic GEM trajectories are in purple and light purple,
669 respectively. The quantitative genetics (QG) expectation is in bold orange. The difference between the
670 evolutionary stable strategy (ESS) and the transient evolutionary attractors (TEAs) can be seen by
671 comparing the dashed orange and pink lines in the second row. Lifetime reproductive success as a
672 function of b_{max} is shown for individuals that were born and died within the last 50 time steps. The
673 evidence that the population evolves toward the TEA is the convergence of the purple line in the second
674 row with the dashed pink line and by looking at the phase portrait in the fifth row. The dashed black line
675 in row three is the average initial trait variance in the population.
676
677 Figure 4. Results of Gillespie eco-evolutionary model (GEM) simulations of the birth-death logistic model
678 for populations culled from a starting population at the ESS trait ($\overline{b_{max}} = 5.4$) and the equilibrium
679 abundance (72 individuals). From left to right, the population is culled more severely (to 50, 30, and 10
680 from left to right). Layout the same as in Figure 3 with 50 replicate simulations. The evidence that the
681 population evolves toward the TEA is the convergence of the purple line in the second row with the
682 dashed pink line and by looking at the phase portrait in the fifth row.
683

684 Figure 1.

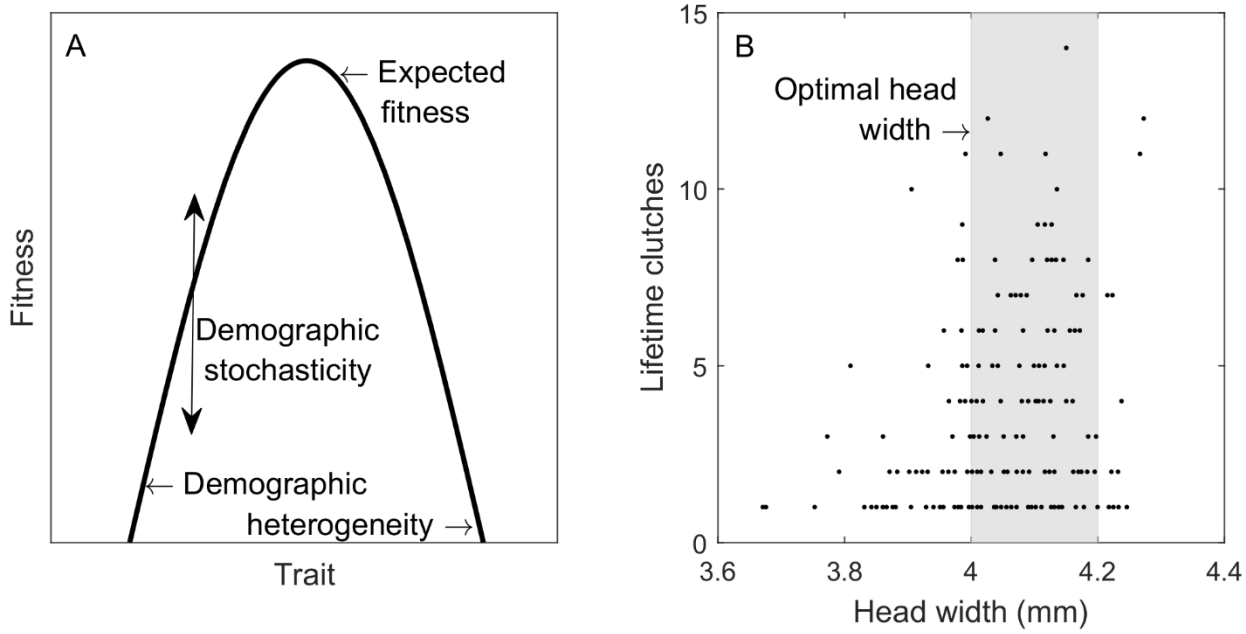

685

686

687 Figure 2.

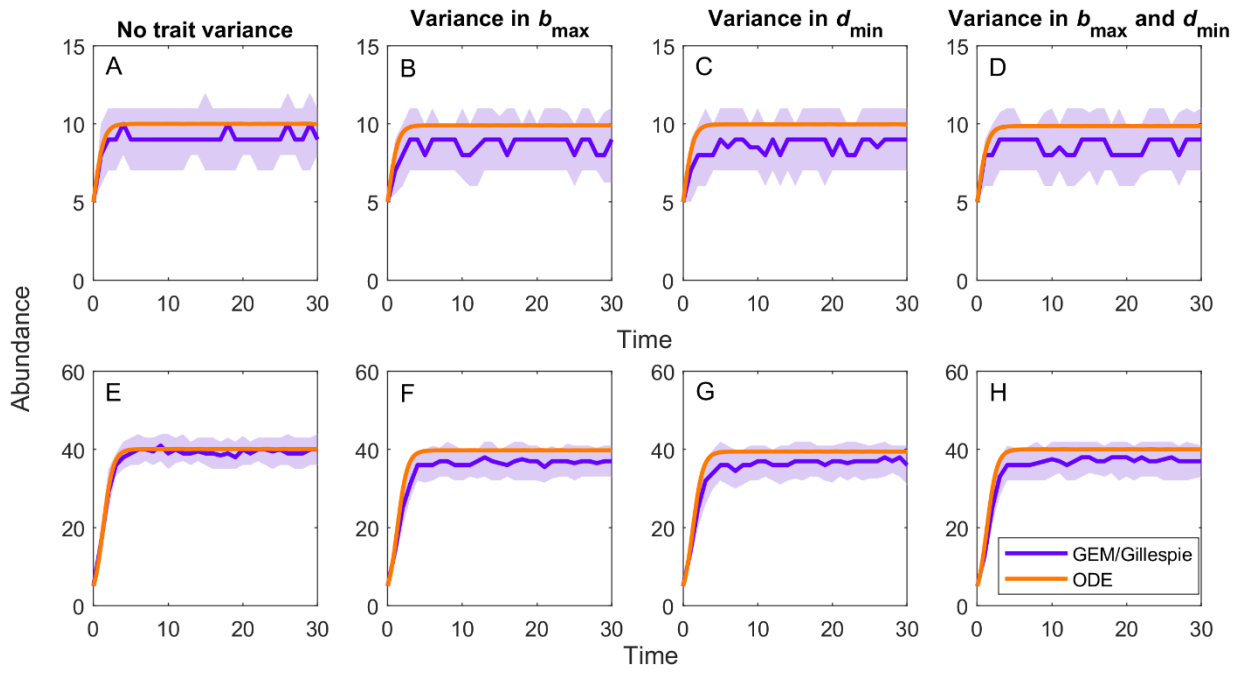

688

689

690 Figure 3.

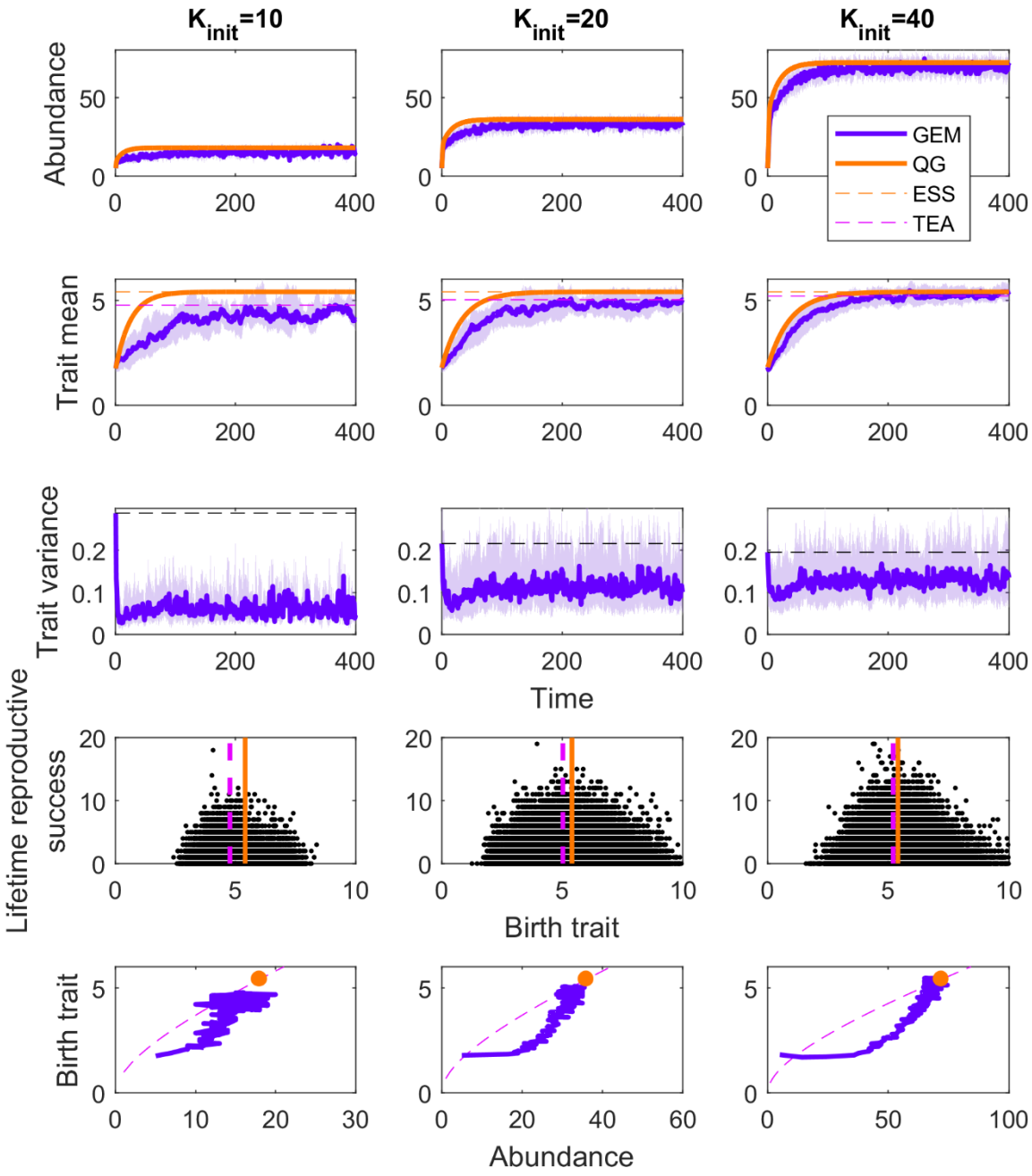

691

692

693 Figure 4.

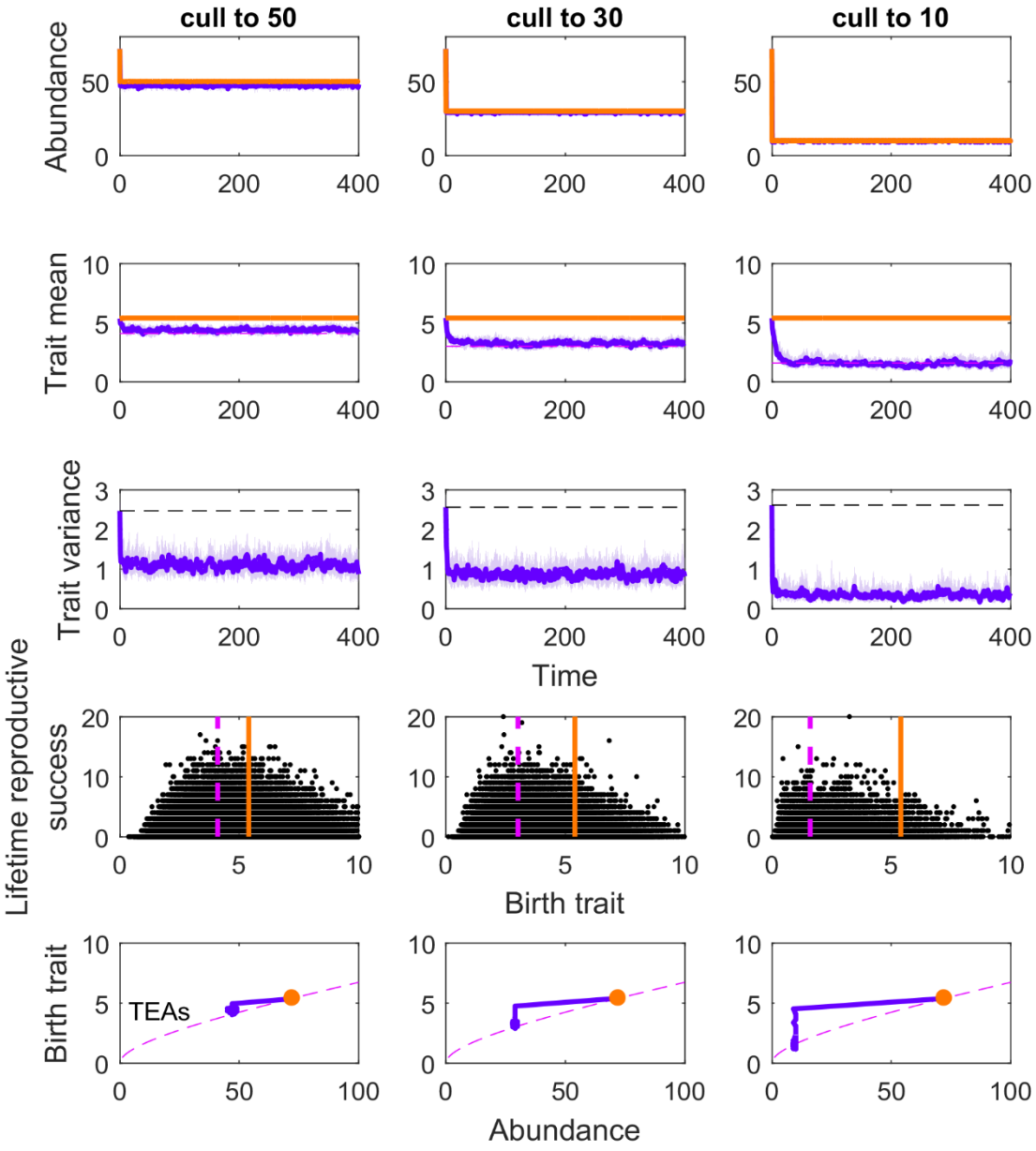

694

695

696

DeLong and Cressler, "Stochasticity directs adaptive evolution toward transient evolutionary attractors"

Appendix S1. Heritability rules.

In a GEM, births and deaths occur through an iterative, stochastic process given an underlying model. In the event of a birth, a new individual is added to the population given some rule for heritability of that trait. In these simulations, we follow the heritability rules derived and presented in (DeLong & Luhring 2018; DeLong & Belmaker 2019) with the change that we are not using here the weighted mean for the parental trait.

If a birth event occurs in a GEM, an offspring trait is randomly drawn from a lognormal distribution with a mean of $\mu_{offspring} = (1 - h^2)\overline{b_{max}} + h^2 b_{max}$, where b_{max} is the actual trait of the current parent, $\overline{b_{max}}$ is the current population mean, and h^2 is narrow-sense heritability. The standard deviation of this distribution is given as $\sigma_{offspring} = \sqrt{(1 - h^{2^2})}[(1 - h^2)\sigma_0 + h^2\sigma_t]$, where σ_0 is the standard deviation in b_{max} in the initial population and σ_t is the standard deviation in b_{max} currently. This trait is then added as a new element of the trait distribution, increasing the size of the population by one and changing the mean and variance of the trait distribution.

This rule is derived from the equation of the regression line in a parent-offspring regression (DeLong & Belmaker 2019). To verify that the realization of this rule in a GEM implementation generates a parent-offspring regression with an estimated h^2 that matches what was set in the model, we track parent and offspring traits through GEMs initialized with different h^2 values (0.9, 0.7, 0.5, and 0.3). Using simple linear regression of offspring traits on

parent traits, we verify that the estimated h^2 (the slope of the regression) remains close to the expected h^2 (Fig. S1-S4).

Over any short interval of time in a GEM run, the realized parent-offspring relationship behaves as expected. After accumulating observations over longer runs, however, we see that the h^2 appears to converge on one. This is also expected: as the population evolves, the parent and offspring traits move in phenotypic space (as you can see from the changing x- and y-axis ranges in Figs. S1-S4), "smearing" the parent-offspring regressions (each of which has a slope of h^2 at any one moment in time) into a parent-offspring regression that has a slope approaching one.

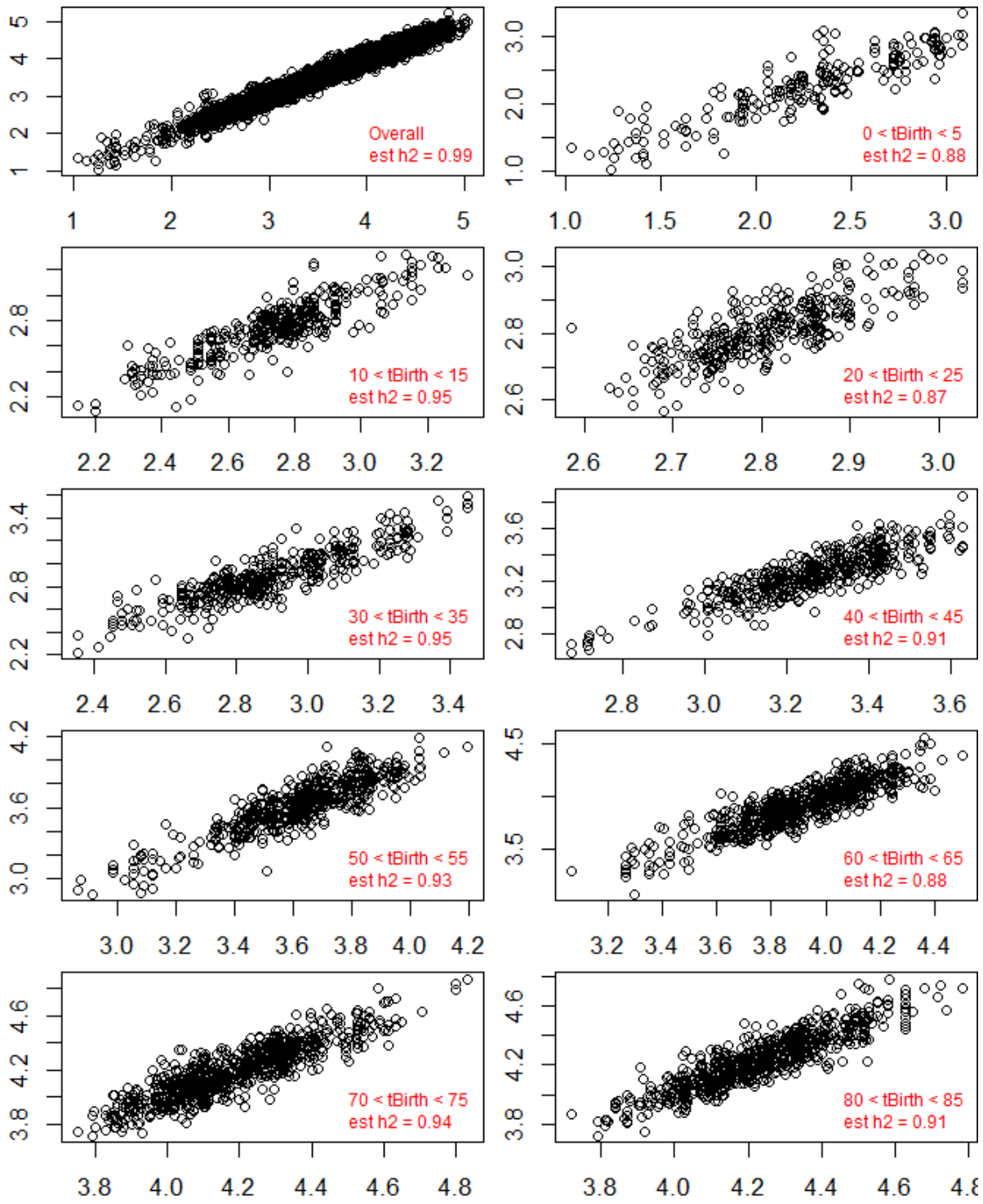

Fig. S1. Parent-offspring regressions through time when $h^2 = 0.9$.

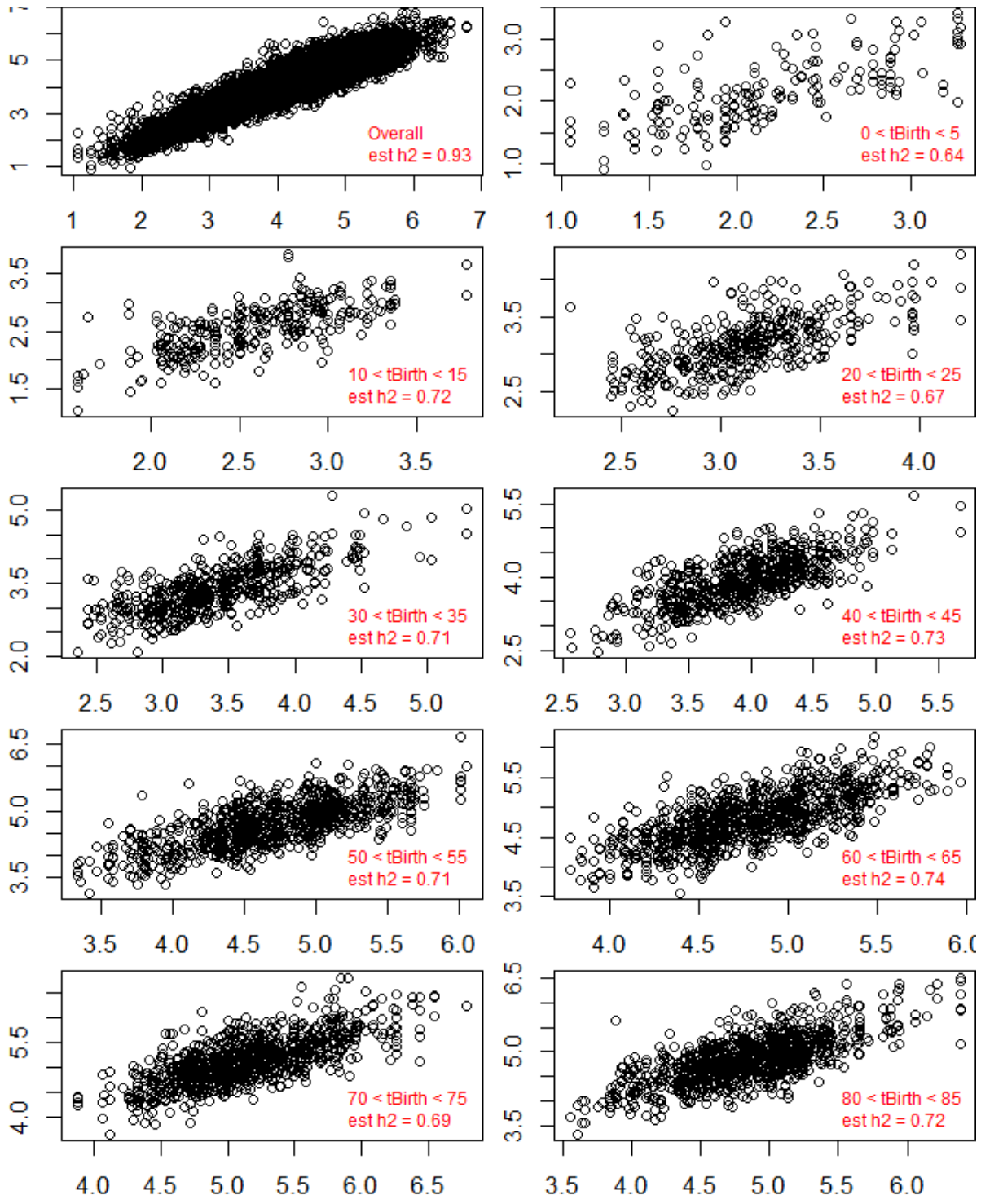

Fig. S2. Parent-offspring regressions through time when h^2 = 0.7.

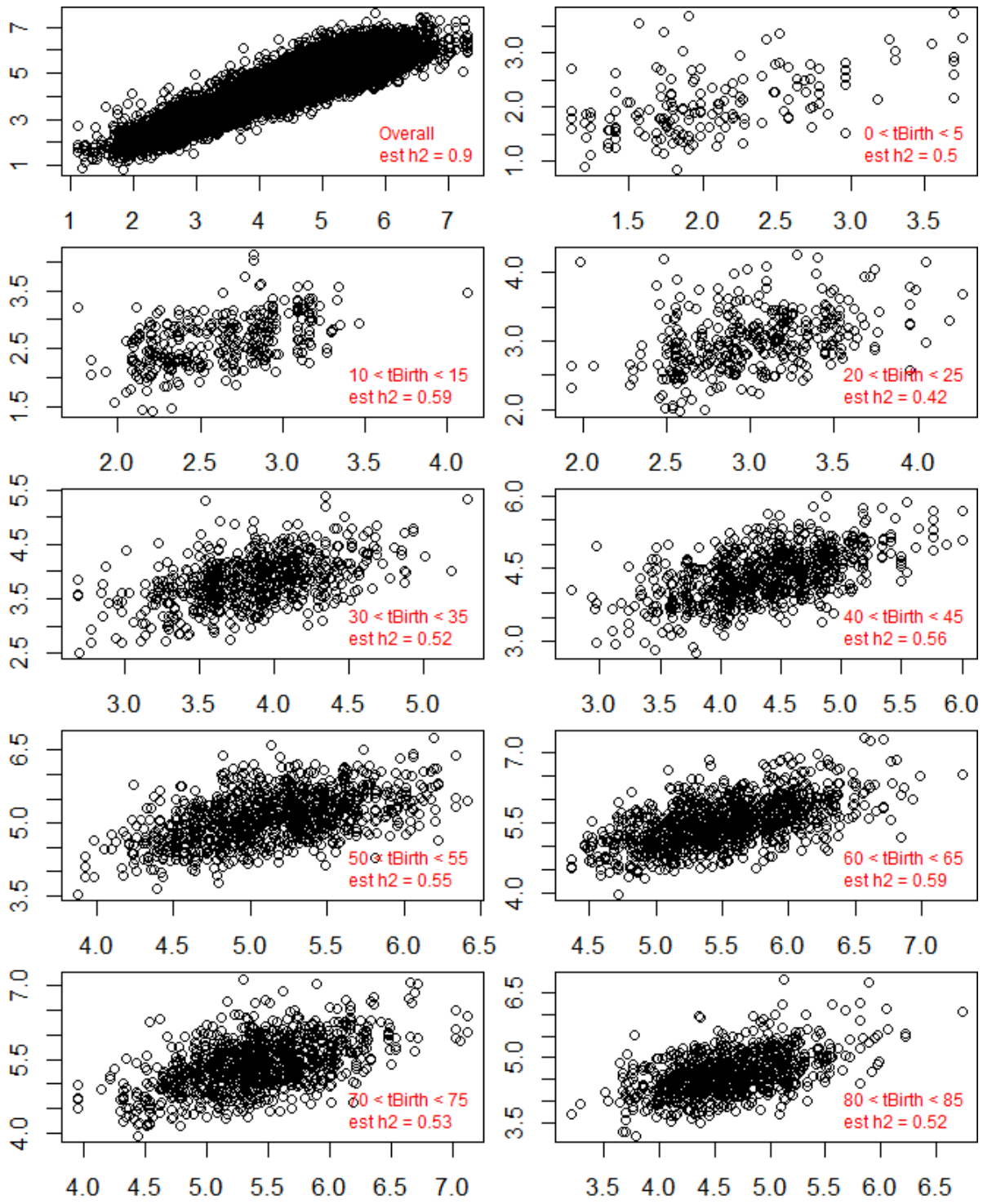

Fig. S3. Parent-offspring regressions through time when $h^2 = 0.5$.

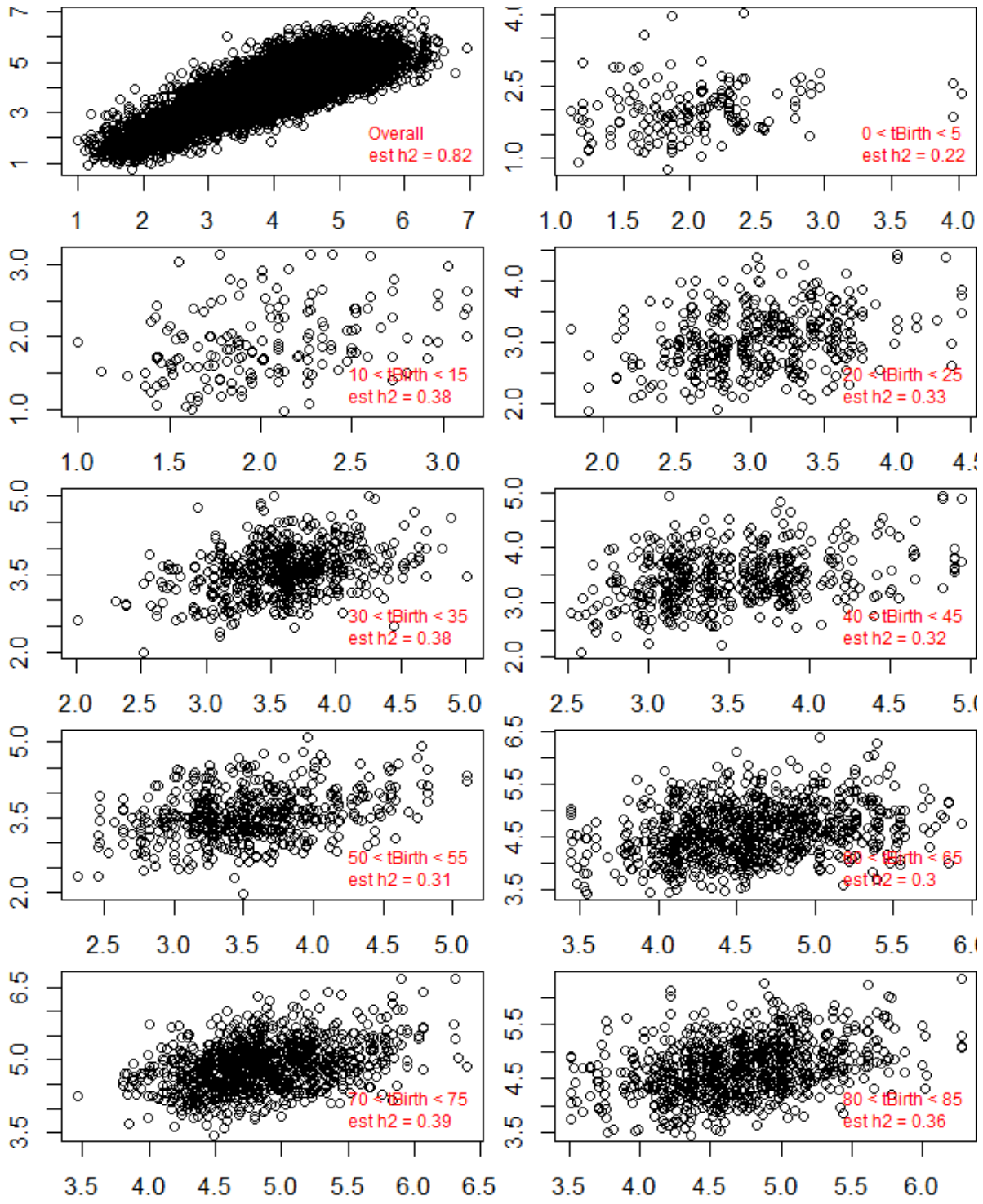

Fig. S4. Parent-offspring regressions through time when h^2 = 0.3.

DeLong and Cressler, "Stochasticity directs adaptive evolution toward transient evolutionary attractors"

Appendix S2. Deriving the evolutionary dynamics for the ecological model with culling

Consider the following ecological model:

$$\frac{dR}{dt} = (b_{max} - b_s R)R - (d_{min} + d_s R)R - x \max(0, R - R_{cull}),$$

where d_{min} is a function of b_{max}.

We will consider two ways of deriving the evolutionary dynamics.

In the first, we follow the approach of (Day & Gandon 2006) and derive an exact model for the evolutionary system. Let us consider our population-level model to a model of *n* "genotypes", $i = \{1,2, \dots, n\}$. The dynamics of each genotype are given by the equation:

$$\frac{dR_i}{dt} = (b_{max,i} - b_s R)R_i - (d_{min,i} + d_s R)R_i - x \max(0, R - R_{cull}) \frac{R_i}{R},$$

where $b_{max,i}$ and $d_{min,i}$ are the birth and death rate of this genotype, $R = \sum_i R_i$ is the total population size, and R_i/R gives the probability that individuals of this genotype will be among those culled if the total population size is larger than R_{cull} (alternatively, you can interpret xR_i/R as the relative rate of culling of R_i).

Absent any process of mutation (e.g., if heritability was perfect), this is a full description of the evolutionary dynamics of the system. The model could be extended to consider mutation between genotypes (or the creation of new genotypes). However, the above system describes selection among the genotypes, which is the key process which we wish to derive here.

We will change variables to track the frequencies of each genotype, $p_i = R_i/R$. Then the dynamics of this frequency will be given by

$$\frac{dp_i}{dt} = \frac{1}{R}\frac{dR_i}{dt} - p_i \frac{1}{R}\frac{dR}{dt}.$$

The dynamics of total population size, $R = \sum_i R_i$, are given by

$$\frac{1}{R}\frac{dR}{dt} = \sum_i \left(b_{max,i}\frac{R_i}{R}\right) - b_s \sum_i R_i - \sum_i \left(d_{min,i}\frac{R_i}{R}\right) - d_s \sum_i R_i - \frac{1}{R}\, x \max(0, R - R_{cull}) \sum_i \left(\frac{R_i}{R}\right)$$

$$\frac{1}{R}\frac{dR}{dt} = \sum_i \left(b_{max,i}\, p_i\right) - b_s R - \sum_i \left(d_{min,i} p_i\right) - d_s R - \frac{1}{R}\, x \max(0, R - R_{cull})$$

$$\frac{1}{R}\frac{dR}{dt} = \overline{b_{max}} - b_s R - \overline{d_{min}} - d_s R - \frac{1}{R}\, x \max(0, R - R_{cull})$$

The sums $\sum_i(b_{max,i}\, p_i)$ and $\sum_i(d_{min,i} p_i)$ are just the average values $\overline{b_{max}}$ and $\overline{d_{min}}$ across all genotypes.

Then the frequency dynamics are given by

$$\frac{dp_i}{dt} = (b_{max,i} - b_s R)p_i - (d_{min,i} + d_s R)p_i - \frac{1}{R}\, x \max(0, R - R_{cull})p_i$$
$$- p_i(\overline{b_{max}} - b_s R - \overline{d_{min}} - d_s R - \frac{1}{R}\, x \max(0, R - R_{cull})$$

$$\frac{dp_i}{dt} = p_i\left(b_{max,i} - \overline{b_{max}} - \left(d_{min,i} - \overline{d_{min}}\right)\right) = p_i\left(\left(b_{max,i} - d_{min,i}\right) - \left(\overline{b_{max}} - \overline{d_{min}}\right)\right)$$
$$= p_i(r_i - \bar{r})$$

Thus, the frequency of each genotype depends on the difference between this genotype's per-capita birth and death rates and the population average birth and death rates. Specifically, if the difference between the maximum birth and minimum death rates for this genotype is larger than the population average, the genotype will increase in frequency.

Given this equation for dp_i/dt, we can derive an equation for the dynamics of the average trait, $\overline{b_{max}} = \sum_i(b_{max,i}\, p_i)$:

$$\frac{d\overline{b_{max}}}{dt} = \sum_i \left(b_{max,i} \frac{dp_i}{dt}\right) = \sum_i \left(b_{max,i}\, p_i r_i\right) - \sum_i \left(b_{max,i}\, p_i \bar{r}\right) = \sum_i \left(b_{max,i}\, p_i r_i\right) - \overline{b_{max}}\, \bar{r}$$

This latter expression is the covariance between b_{max} and r across all strains; that is,

$$\frac{d\overline{b_{max}}}{dt} = \mathrm{cov}(b_{max}, r)$$

This is Price's equation (Day & Gandon 2006). Assuming normality of the phenotype distribution, (Taylor & Day 1997) show that the covariance is proportional to the product of the additive genetic variance and fitness gradient (the derivative of individual fitness with respect to the individual trait (Abrams 2001), implying that the evolutionary dynamic can be written as

$$\frac{d\overline{b_{max}}}{dt} = V\left(\frac{\partial r}{\partial b_{max}}\right)_{b_{max}=\overline{b_{max}}}$$

Since $= b_{max} - d_{min} = b_{max} - c b_{max}^2$, $\frac{\partial r}{\partial b_{max}} = 1 - 2c b_{max}$, and the evolutionary dynamic in the model with culling is identical to the evolutionary model without culling.

Note: GEMs actually assume that the trait is actually *lognormally* distributed, to prevent negative trait values. This modifies the above derivation only slightly. In particular, $\log(\overline{b_{max}}) = \log(\sum_i(b_{max,i}\, p_i))$, so the trait dynamics would be given by:

$$\frac{d\log(\overline{b_{max}})}{dt} = \frac{1}{\overline{b_{max}}} \sum_i \left(b_{max,i} \frac{dp_i}{dt}\right) = \frac{\mathrm{cov}(b_{max}, r)}{\overline{b_{max}}} = \frac{V}{\overline{b_{max}}}\left(\frac{\partial r}{\partial b_{max}}\right)_{b_{max}=\overline{b_{max}}}.$$

Thus the direction of evolution (and equilibrium) of a lognormally distributed trait will be identical to that of a normally distributed trait, although the rate will differ because of the normalization by the mean trait.

We can also show this using more of an adaptive dynamics approach. That is, consider the invasion of a mutant with a different b_{max} value into a monomorphic resident population. Let $b_{max,m}$ and $b_{max,r}$ be the mutant and resident trait values, respectively. Then the dynamics of the two populations are given by

$$\frac{dR_r}{dt} = (b_{max,r} - b_s(R_r + R_m))\, R_r - (d_{min,m} + d_s(R_r + R_m))R_r - x \max(0, (R_r + R_m - R_{cull}) \frac{R_r}{R_m + R_r}$$

$$\frac{dR_m}{dt} = (b_{max,m} - b_s(R_r + R_m))\, R_m - (d_{min,m} + d_s(R_r + R_m))R_m - x \max(0, R_r + R_m - R_{cull}) \frac{R_m}{R_m + R_r}$$

If we assume that the mutant is attempting to invade from rarity (so $R_m = 0$), then whether it will be able to invade will be given by the stability of the equilibrium $\left(R_r = \widehat{R_r}, R_m = 0\right)$. The stability can be assessed with the Jacobian matrix

$$\begin{pmatrix} \frac{\partial\left(\frac{dR_r}{dt}\right)}{\partial R_r} & \frac{\partial\left(\frac{dR_r}{dt}\right)}{\partial R_m} \\ \frac{\partial\left(\frac{dR_m}{dt}\right)}{\partial R_r} & \frac{\partial\left(\frac{dR_m}{dt}\right)}{\partial R_m} \end{pmatrix}_{R_r = \widehat{R_r}, R_m = 0}$$

$$= \begin{pmatrix} \left(b_{max,r} - b_s R_r\right) - \left(d_{min,m} + d_s R_r\right) - x & \frac{\partial\left(\frac{dR_r}{dt}\right)}{\partial R_m} \\ 0 & (b_{max,m} - b_s R_r) - (d_{min,m} + d_s R_r) - \frac{x}{R_r} \max(0, R_r - R_{cull}) \end{pmatrix}$$

Since this matrix is upper-triangular, the eigenvalues are given along the diagonal. The first eigenvalue determines the stability of the system when the mutant is absent, and we can assume it is negative. Therefore, the mutant can invade if the following is satisfied:

$$r_{max,r,cull} = (b_{max,m} - b_s R_r) - (d_{min,m} + d_s R_r) - \frac{x}{R_r} \max(0, R_r - R_{cull}) > 0.$$

The quantity $r_{max,r,cull}$ is often termed the "invasion fitness" (Geritz *et al.* 1998), and the derivative of this expression with respect to the mutant trait $\frac{\partial r_{max,r,cull}}{\partial b_{max,m}}$, evaluated at the value $b_{max,m} = b_{max,r}$ (consistent with the adaptive dynamics assumption that mutations are small), determines the direction

of selection. It is clear that $\left(\frac{\partial r_{max,r,cull}}{\partial b_{max,m}}\right)_{b_{max,m}=b_{max,r}} = 1 - 2cb_{max,r}$. This is identical to the expression derived above, as expected given that the fitness gradient expressions between QG and AD approaches are often identical (Abrams *et al.* 1993c; Dieckmann & Law 1996; Taylor & Day 1997; Abrams 2001; Doebeli *et al.* 2017). This serves as further confirmation that the evolutionary equilibrium will be independent of culling.

References

Abrams. (2001). Modelling the adaptive dynamics of traits involved in inter- and intraspecific interactions: An assessment of three methods. Ecology Letters, 4, 166–175.

Abrams, P.A., Matsuda, H. & Harada, Y. (1993). Evolutionarily unstable fitness maxima and stable fitness minima of continuous traits. Evol Ecol, 7, 465–487.

Day, T. & Gandon, S. (2006). Insights from Price's equation into evolutionary epidemiology. Disease evolution: models, concepts, and data analyses, 71, 23.

Dieckmann, U. & Law, R. (1996). The dynamical theory of coevolution: a derivation from stochastic ecological processes. J Math Biol, 34, 579–612.

Doebeli, M., Ispolatov, Y. & Simon, B. (n.d.). Towards a mechanistic foundation of evolutionary theory. eLife, 6.

Geritz, S.A.H., Kisdi, E., Mesze´NA, G. & Metz, J.A.J. (1998). Evolutionarily singular strategies and the adaptive growth and branching of the evolutionary tree. Evolutionary Ecology, 12, 35–57.

Taylor, P. & Day, T. (1997). Evolutionary stability under the replicator and the gradient dynamics. Evol Ecol, 11, 579–590.

DeLong and Cressler, "Stochasticity directs adaptive evolution toward transient evolutionary attractors"

Appendix S3. Supplementary results

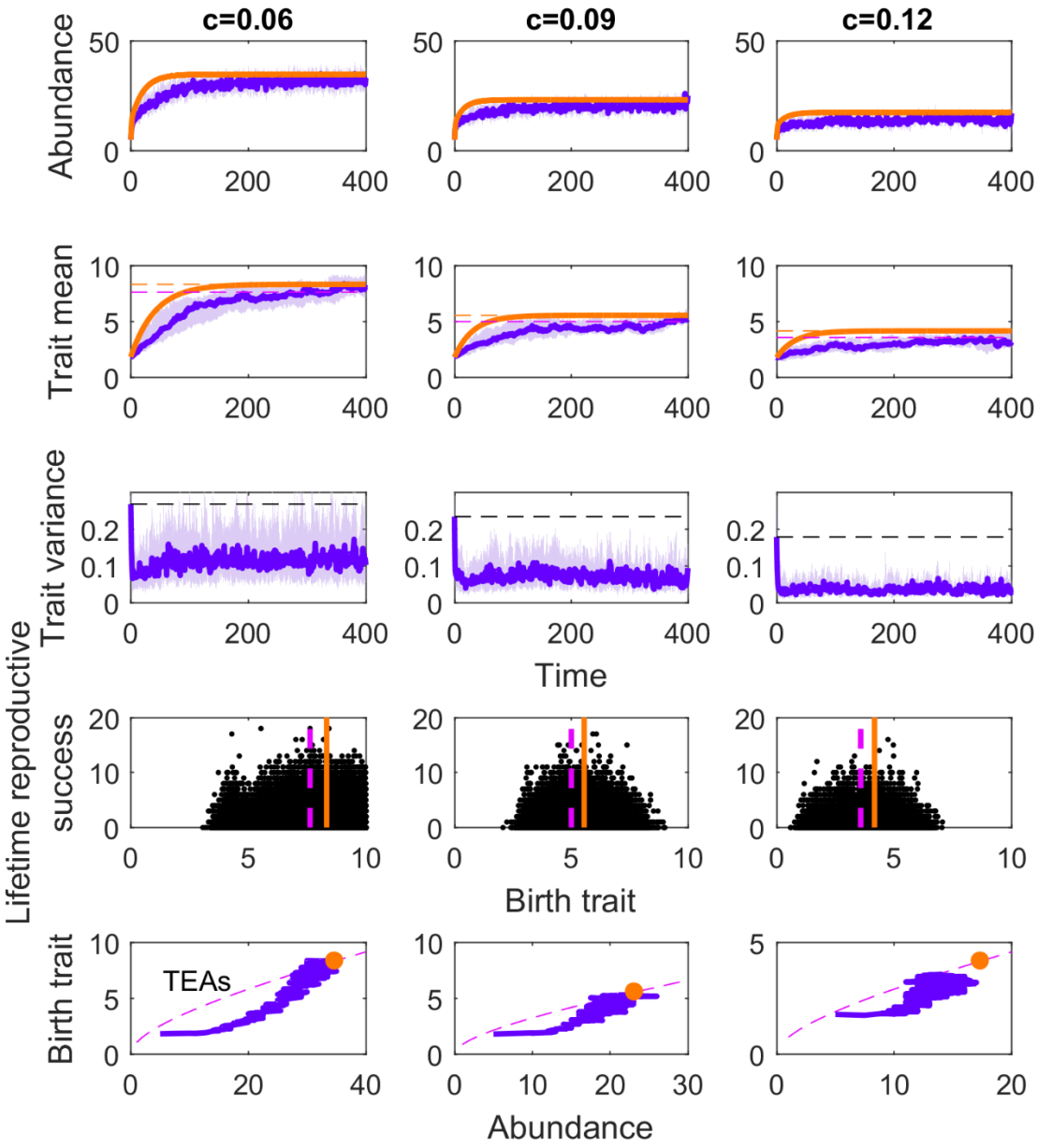

Figure S5. . Gillespie eco-evolutionary model (GEM) simulations of the birth-death logistic model. The rows show from top to bottom population abundance, mean maximum rate of births (b_{max}), variance in b_{max}, lifetime reproductive success (product of expected births and expected lifespan), and the mean

trajectory through the abundance- b_{max} phase plane. The columns show three levels of the trade-off constant between b_{max} and d_{min} (c = 0.06, 0.09, and 1.2 from left to right). Other parameters include b_s = d_s = 0.04, CV of b_{max} in the initial population was 0.3, and heritability (h^2) was 0.75. The median and middle 50% of 50 stochastic GEM trajectories are in purple and light purple, respectively. The quantitative genetics (QG) expectation is in bold orange. The difference between the evolutionary stable strategy (ESS) and the transient evolutionary attractors (TEAs) can be seen by comparing the dashed orange and pink lines in the second row. Lifetime reproductive success as a function of b_{max} is shown for individuals that were born and died within the last 50 time steps. The evidence that the population evolves toward the TEA is the convergence of the purple line in the second row with the dashed pink line and by looking at the phase portrait in the fifth row.